ARTICLES

Quantum Mechanical Study of the Photoisomerizations of Bicyclo[4,1,0]hept-2-ene (2-Norcarene)

Ming-Der Su*

Department of Applied Chemistry, National Chiayi University, Chiayi 60004, Taiwan

Received: April 18, 2008; Revised Manuscript Received: October 15, 2008

The mechanisms of the photochemical isomerization reactions were investigated theoretically using a model system of bicyclo[4,1,0]hept-2-ene (2-norcarene) **1** with the CASSCF (eight-electron/eight-orbital active space) and MP2-CAS methods and the 6-311(d) basis set. The structures of the conical intersections and intersystem crossings, which play a crucial role in such photoisomerization reactions, were obtained. The intermediates and transition structures of the ground-state were also calculated to assist in providing a qualitative explanation of the reaction pathways. Our model investigations suggest that the preferred singlet photoreaction route for **1** is as follows: singlet reactant → Franck−Condon region → conical intersection → intermediate → transition state → photoproduct. On the other hand, our theoretical findings indicate that the preferred triplet photoreaction route for **1** is as follows: singlet reactant → Franck−Condon region → triplet minimum → triplet transition state → intersystem crossing → intermediate → singlet transition state → photoproduct. In particular, the intersystem crossing mechanism found in this work gives a better explanation and supports the available experimental observations. Two kinds of reaction pathways, which can lead to final photoproducts, have been identified: (paths I or III) ring-expansion to form a cycloheptene ring and (paths II or IV) ring-closure to form a methylcyclohexene structure. Both exhibit biradical character. Also, our theoretical investigations strongly indicate that substantial interaction occurs between the cyclopropane moiety and the isolated carbon−carbon double bond in the excited state of (**1**).

I. Introduction

Intramolecular photochemical interaction between two chromophoric units bridged by more than one bond has been of great interest to both experimental and theoretical chemists.[1] Many experimental studies concerning saturated mono-[2] and polycyclic[3] derivatives as well as rigid[4] and semirigid[5] nonconjugated bichromophoric systems have demonstrated that some interaction between the cyclopropane moiety and the isolated carbon−carbon double bond is possible. However, in contrast to the photochemistry generally observed in aliphatic cyclopropanes,[2−5] or even in other vinylcyclopropane derivatives,[1b] the product mixture observed upon direct irradiation of bicyclo[4,1,0]hept-2-ene[6] (**1**, 2-norcarene) reveals that this system is unusual as shown in Scheme 1.[7] Also, it was pointed out that the product distribution is independent of both solvent and excitation wavelength and is unchanged by the addition of naphthalene.[6]

It is these fascinating experimental results that have inspired this study. The calculation of reaction pathways for such photoisomerizations of 2-norcarene and the location and identification of the structures of the crucial points are therefore of great academic interest. In fact, an understanding of the detailed mechanism of such photoreactions is essential to the rationalization of the mechanisms of intramolecular photochemical isomerizations, which are useful in synthetic chemistry. Theoretical methods are the only techniques for determining the properties of the various excited-state potential-energy surfaces. Nevertheless, to the best of our knowledge, until now no theoretical work has been devoted to the study of the photochemistry of such a vinylcyclopropane derivative (2-norcarene). We have thus undertaken the theoretical investigation of the potential-energy surfaces of the 2-norcarene system.

SCHEME 1

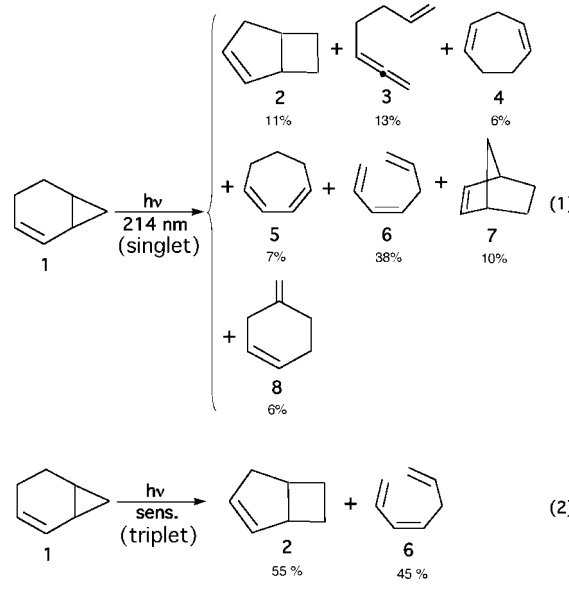

* To whom correspondence should be addressed. E-mail: midesu@mail.ncyu.edu.tw.

10.1021/jp803365u CCC: $40.75
Published on Web 12/18/2008

SCHEME 2

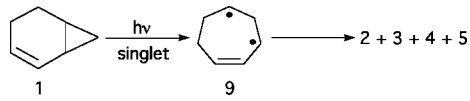

SCHEME 3

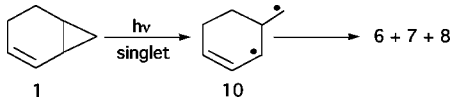

The object of the present work is to gain an understanding of the photochemical mechanism of the isomerization reactions of 2-norcarene. As discussed below, the mechanisms of various reactions were investigated by CASSCF and MP2-CAS calculations. Bicyclo[4,1,0]hept-2-ene (**1**) was therefore used as a model system. It will be shown later that conical intersections and intersystem crossings[8] play a crucial role in the photoisomerization of the vinylcyclopropane derivative (2-norcarene) system. From these investigations, a better understanding of the thermodynamic and kinetic aspects of such vinylcyclopropane photoreactions may shed some light on the optimal design of further related synthesis and catalytic processes.

II. Methodology

All of the geometries were fully optimized without imposing any symmetry constraints, although in some instances the resulting structures showed various elements of symmetry. The complete-active-space SCF (CASSCF) calculations were performed using the *MCSCF* program released in *Gaussian 03*.[9]

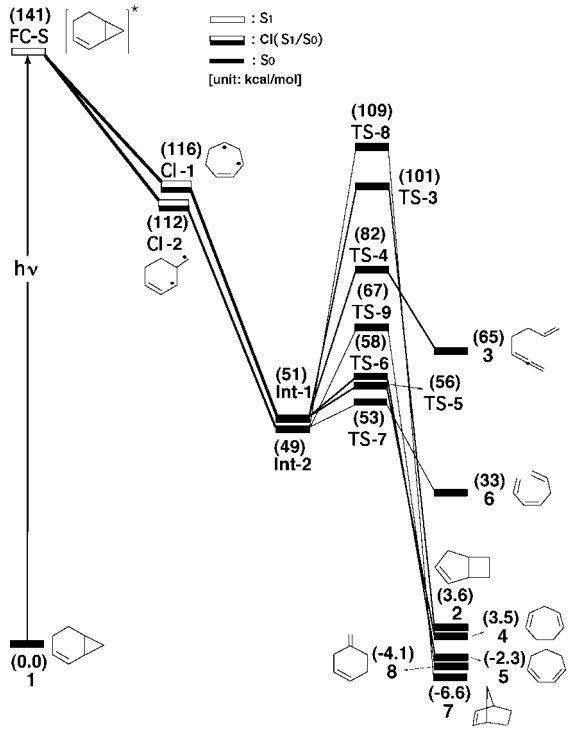

Figure 1. Singlet-energy profiles for the photoisomerization modes of bicyclo[4,1,0]hept-2-ene (**1**). The abbreviation FC stands for Frank−Condon. The relative energies were obtained at the MP2-CAS(8,8)/6-311G(d)//CAS(8,8)/6-311G(d) and CAS(8,8)/6-311G(d) (in parentheses) levels of theory. All energies (in kcal/mol) are given with respect to the reactant (**1**). For the CASSCF optimized structures of the crucial points, see Figures 2−4. For more information, see the text.

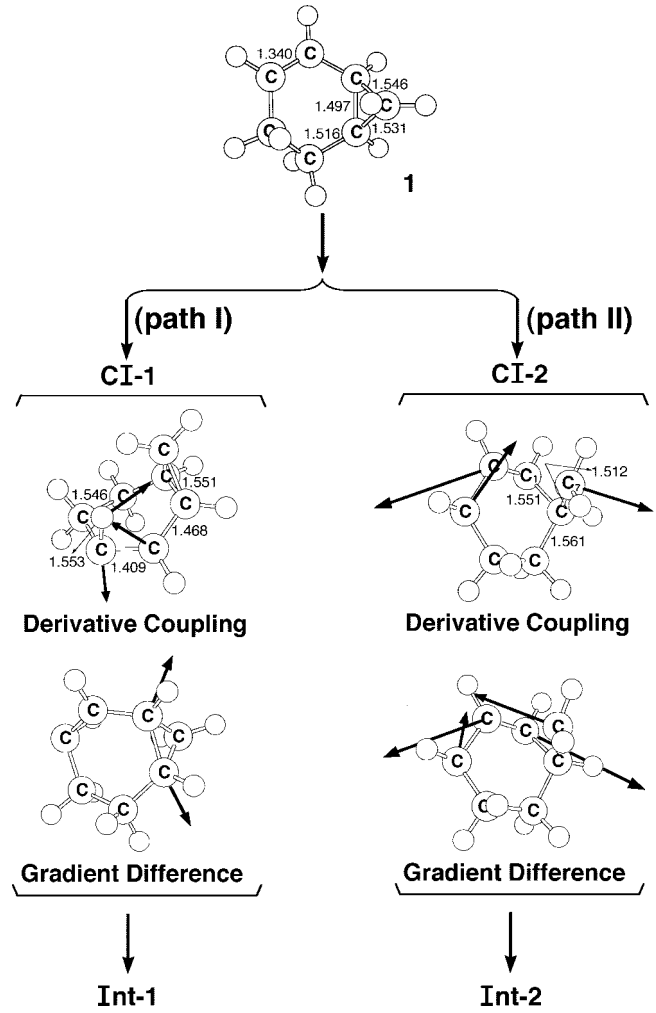

Figure 2. CAS(8,8)/6-311G(d) geometries (in angstroms and degrees) for path I and path II of bicyclo[4,1,0]hept-2-ene (**1**). These paths include conical intersections (**CI-1** and **CI-2**). The corresponding CASSCF vectors are shown in the inset. For more information, see the Supporting Information.

In the investigation of photochemical reaction pathways, the stationary point structures on the S_0, S_1, and T_1 surfaces were optimized at the CASSCF level of calculation using the standard 6-311G(d) basis set.[10] The active space for describing the photoisomerizations of bicyclo[4,1,0]hept-2-ene (**1**) comprises eight electrons in eight orbitals, that is, two p-π orbitals plus three σ(C−C) and σ^*(C−C) orbitals. In some cases (such as the hydrogen migration reaction), an active space comprising eight electrons in eight orbitals (π, σ, σ, π^*, σ^*, σ^* in the cycloheptene ring, and the σ, σ^* orbitals in the C−H bond) was used. Therefore, the state-averaged CASSCF(8,8) method was used to determine geometry in the intersection space.

Every stationary point was characterized by its harmonic frequencies computed analytically at the CASSCF level. The harmonic vibrational frequencies of all stationary points were computed analytically to characterize them as minima (all frequencies are real) or transition states (only one imaginary frequency). The optimization was terminated when the maximum force and its root mean square were less than 0.00045 and 0.00005 hartree/bohr, respectively. Localization of the minima, transition states, and crossing minima have been performed in Cartesian coordinates; therefore, the results are independent of any specific choice of internal variables.

To correct the energetics for dynamic electron correlation, we have used the multireference Møller−Plesset (MP2-CAS)

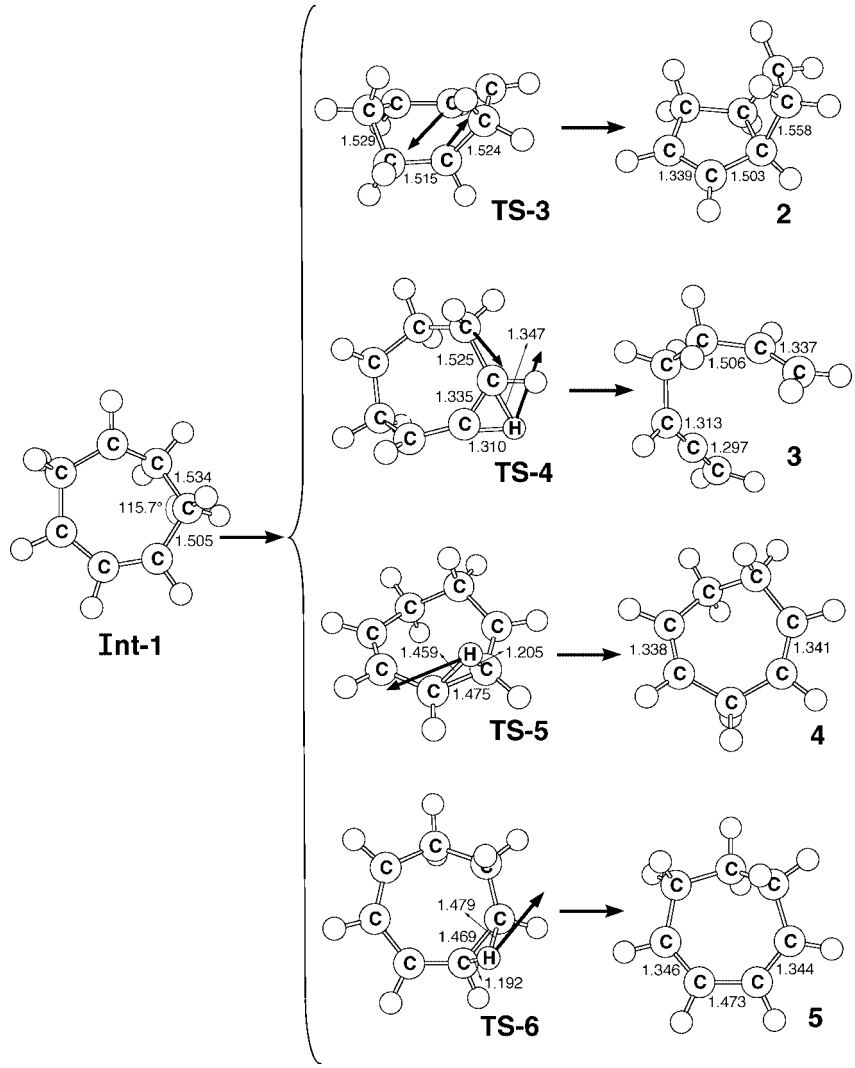

Figure 3. CAS(8,8)/6-311G(d) geometries (in angstroms and degrees) for paths I-1, I-2, I-3, and I-4 of bicyclo[4,1,0]hept-2-ene (**1**), intermediate (**Int-1**), transition states (**TS-3**, **TS-4**, **TS-5**, and **TS-6**) and isomer products (**2**, **3**, **4**, and **5**, respectively). The heavy arrows indicate the main atomic motions in the transition-state normal modes. For more information, see the Supporting Information.

algorithm[11] as implemented in the program package *Gaussian 03*. Unless otherwise noted, the relative energies given in the text are those determined at the MP2-CAS-(8,8)/6-311G(d) level using the CAS(8,8)/6-311G(d) (hereafter designated MP2-CAS and CASSCF, respectively) geometry.

III. General Consideration

As already illustrated in Scheme 1, the bicyclo[4,1,0]hept-2-ene (**1**, 2-norcarene) photoisomerization reported experimentally[6] shows a wide variety of reaction types. However, it is still possible to construct a certain consistency among these reactions, which at least serves as a basis for discussion. In this section, we describe possible excited-state reaction paths that lead to conical intersections or intersystem crossings. A schematic representation of the relationships between the intersections and possible reaction routes are shown in Schemes 2 and 3.

In the case of the singlet photochemistry of bicyclo[4,1,0]hept-2-ene (eq 1),[6] the most reasonable pathway for the conversion of **1** to **2**, **3**, **4**, and **5** is via an internal bond (C_1 and C_6) cleavage of the cyclopropane ring, which can be represented as shown in **9**. That is, one cyclopropane bond will be opened to form a cyclic biradical species **9** (Scheme 2). It should be noted that this mechanism implies that some interaction between the isolated double bond and the cyclopropane chromophore should occur.

Moreover, 2-norcarene, **1**, displays an intriguing type of reaction upon singlet photolysis, that is, photoisomerization to products **6**, **7**, and **8** (eq 1).[6] This experimental fact strongly suggests the involvement of a 1,3-biradical species (**10**), which subsequently undergoes conical intersection to give the singlet ground-state products. At this point, two-ring closure or 1,2-hydrogen migration provide straightforward routes to **6**, **7**, or **8**, as seen in Scheme 3. Also, Scheme 2 (singlet) and Scheme 3 (singlet) display similar reaction patterns for triplet photochemistry of bicyclo[4,1,0]hept-2-ene **1** (eq 2).[6] That is to say, the intersystem crossing of triplet photochemistry of bicyclo-[4,1,0]hept-2-ene will follow similar mechanisms as the singlet corresponding molecule.

We shall use the above mechanisms (Schemes 2 and 3) in the following sections to locate the funnel from either the excited singlet or triplet-state surfaces to the ground singlet-state surface that corresponds to a conical intersection or an intersystem crossing, respectively.

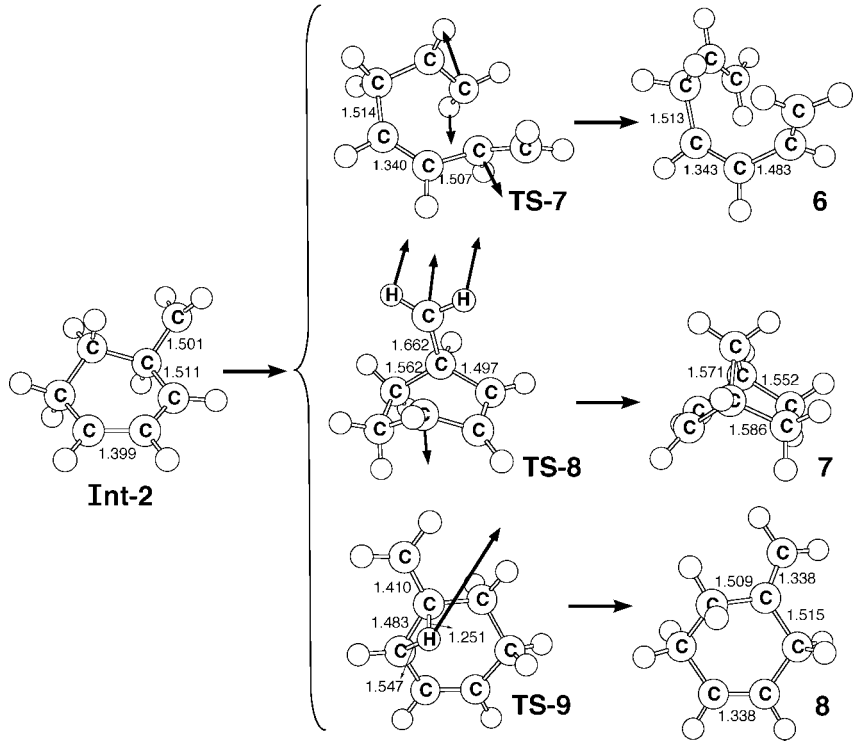

Figure 4. CAS(8,8)/6-311G(d) geometries (in angstroms and degrees) for paths II-1, II-2, and II-4 of bicyclo[4,1,0]hept-2-ene (**1**), intermediate (**Int-2**), transition states (**TS-7**, **TS-8**, and **TS-9**) and isomer products (**6**, **7**, and **8**, respectively). The heavy arrows indicate the main atomic motions in the transition-state normal modes. For more information, see the Supporting Information.

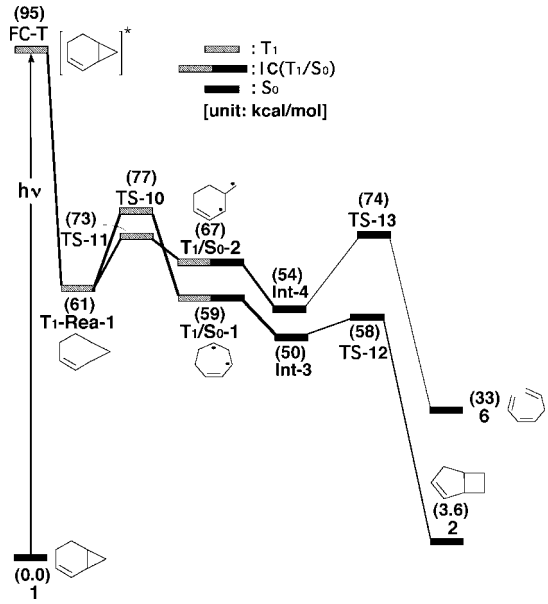

Figure 5. Triplet energy profiles for the photoisomerization modes of bicyclo[4,1,0]hept-2-ene (**1**). The abbreviation FC stands for Frank−Condon. The relative energies were obtained at the MP2-CAS-(8,8)/6-311G(d)// CAS(8,8)/6-311G(d) and CAS(8,8)/6-311G(d) (in parentheses) levels of theory. All energies (in kcal/mol) are given with respect to the reactant (**1**). For the CASSCF optimized structures of the crucial points, see Figures 6 and 7. For more information, see the text.

IV. Results and Discussion

1. Singlet Reaction Mechanisms of Bicyclo[4,1,0]hept-2-ene. Let us first consider the singlet reaction mechanisms of bicyclo[4,1,0]hept-2-ene (**1**). Figure 1 displays the relative energies on the singlet potential-energy surface along the assumed photoisomerization pathways from **1** to various photoproducts (**2**−**8**). Selected optimized geometrical parameters for the critical points of eq 1 and their energies on the ground- and excited singlet-state surfaces can be taken from Figures 2−4, respectively. Cartesian coordinates calculated for the stationary and crossing points at the CASSCF/6-311G(d) level are available as Supporting Information.

In the first step, the reactant (**1**) is excited to its excited singlet state (S_1) by a vertical excitation. After the vertical excitation process the molecule is situated on the singlet surface but still possesses the ground-state (S_0) geometry. This point on the singlet surface is denoted as **FC-S** (S_1 (S_0 geometry)). The computed singlet vertical excitation energy of **1** is 141 kcal/mol ($S_0 \rightarrow S_1$ (S_0 geometry)). Comparison with the corresponding experimental value of 214 nm[6] (= 134 kcal/mol in energy) indicates that the present calculations provide a good estimate of the relative energies for the 2-norcarene system.

From the point reached by the vertical excitation (**FC-S**), the molecule relaxes to reach an S_1/S_0 conical intersection where the photoexcited system decays nonradiatively to S_0. Namely, the photochemically active relaxation path starting from the $S_1^1(\pi \rightarrow \pi^*)$ excited-state of **1** leads to the S_1/S_0 **CI-1** and **CI-2**, which are shown on the right-hand (path I and path II) side of Figure 1, respectively. Both **CI-1** and **CI-2** structures optimized at the CASSCF/6-311G(d) level are shown in Figure 2. The derivative coupling and gradient difference vectors obtained at the conical intersections are also given in Figure 2.

For path I, the system can access a biradical cycloheptene intermediate **Int-1** (Figure 1) via the **CI-1** point. The optimized structures (along with selected bond parameters) of singlet state **Int-1** are given in Figure 3. It should be emphasized that the geometrical structure of **Int-1** is consistent with the previously proposed mechanism shown in Scheme 2, in which the monocyclic intermediate (**9**) bears a double bond and has a biradical character. Moreover, this monocyclic species (**Int-1**) is expected to have a short lifetime before ring rearrangement to the final photoproducts occurs. With regard to the structure

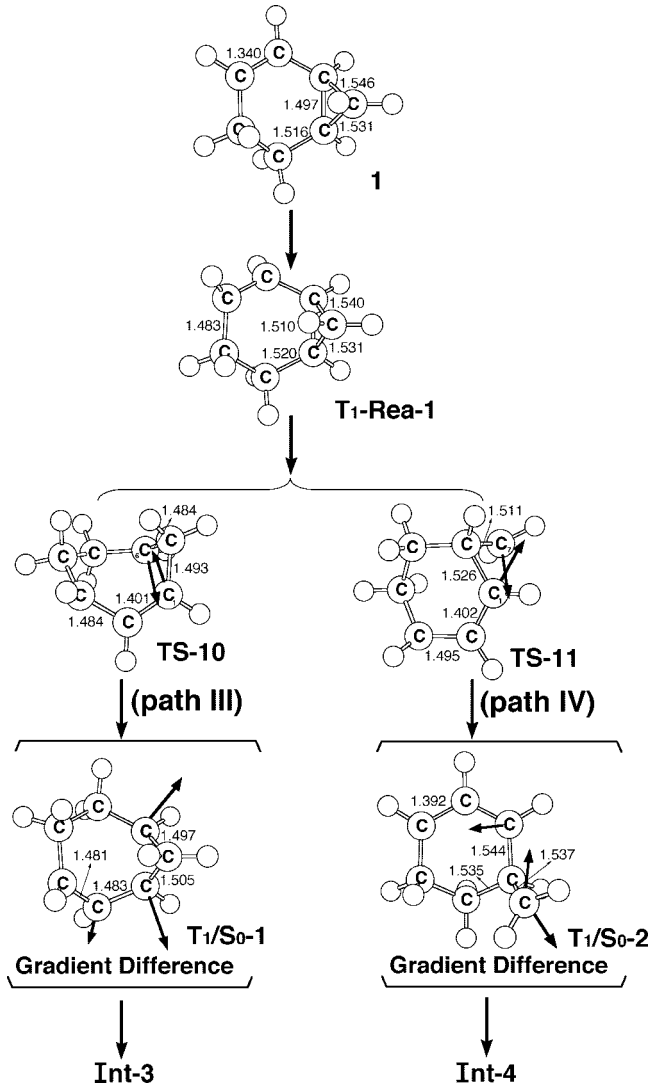

Figure 6. CAS(8,8)/6-311G(d) geometries (in angstroms and degrees) for paths III and IV of bicyclo[4,1,0]hept-2-ene (**1**). These paths include triplet transition states (**TS-10** and **TS-11**) and intersystem crossings (**T1/S0−1** and **T1/S0−2**). The corresponding CASSCF vectors are shown in the inset. For more information, see the Supporting Information.

of **Int-1**, the search for transition states on the S_0 surface gives **TS-3**, **TS-4**, **TS-5**, and **TS-6** for reaction path I-1, path I-2, path I-3, and path I-4, respectively. Our theoretical computations at the CASSCF(8,8) level give imaginary frequencies of 1729*i* (**TS-3**), 3180*i* (**TS-4**), 1727*i* (**TS-5**), and 1775*i* (**TS-6**) cm^{-1}, respectively. These connections (between **Int-1** and corresponding photoproducts) have been verified by moving in both directions from transition states (**TS-3**, **TS-4**, **TS-5**, and **TS-6**; Figure 1) along the intrinsic reaction coordinate.[13]

For path I-1, ring closure to a bicyclic product, bicyclo[3.2.0]hept-2-ene (**2**), will occur via an intramolecular carbon−carbon closing (**TS-3**). Alternatively, a ring-opening isomerization leads to 1,2,6-heptatriene (**3**) by way of an intramolecular 1,2-hydrogen migration between two carbon atoms, accompanied by a C−C bond breaking (**TS-4**). On the other hand, inspection of the normal modes for **TS-5** and **TS-6** shows clearly that these reactions proceed toward formation of monocyclic dienes (1,4-cycloheptadiene **4** and 1,3-cycloheptadiene **5**, respectively). Our theoretical investigations indicate that the barrier heights for these transition states decrease in the order **TS-3** (52 kcal/mol) > **TS-4** (32 kcal/mol) > **TS-6** (8.7 kcal/mol) > **TS-5** (6.9 kcal/mol). Accordingly, our theoretical investigations suggest that paths I-1, I-2, I-3, and I-4 proceed as follows:

$$1(S_0) + h\nu \rightarrow \text{FC-S} \rightarrow \text{CI-1} \rightarrow \text{Int-1} \rightarrow \text{TS-3} \rightarrow 2 \quad (1)$$

$$1(S_0) + h\nu \rightarrow \text{FC-S} \rightarrow \text{CI-1} \rightarrow \text{Int-1} \rightarrow \text{TS-4} \rightarrow 3 \quad (2)$$

$$1(S_0) + h\nu \rightarrow \text{FC-S} \rightarrow \text{CI-1} \rightarrow \text{Int-1} \rightarrow \text{TS-5} \rightarrow 4 \quad (3)$$

$$1(S_0) + h\nu \rightarrow \text{FC-S} \rightarrow \text{CI-1} \rightarrow \text{Int-1} \rightarrow \text{TS-6} \rightarrow 5 \quad (4)$$

Alternatively, our computations suggest that the **CI-2** point can relax to the **Int-2** point via a short energy relief as shown in Figure 1. The fully optimized structure of the singlet state (**Int-2**) is given in Figure 4. As one can see, the molecule at the **Int-2** point has a methylcycloheptene-like structure with two unpaired electrons lying on two different carbon atoms (C_1 and C_7). Again, the geometrical structure of **Int-2** is consistent with the previously proposed mechanism given in Scheme 3 (i.e **10**). Additionally, the calculated energy of **Int-2** is given in Figure 1, from which one can see that its energy is lower than that of the **CI-2** species by 63 kcal/mol. From **Int-2**, isomerization to the final photoproducts (**6**, **7**, and **8**) also involves three reaction pathways (paths II-1, II-2, and II-3, respectively) as shown in Figure 1. That is, the system may undergo a carbon−carbon bond breaking between C_1 and C_6 atoms via a transition state **TS-7** (path II-1). On the other hand, the reaction could proceed via a ring closure and 1,2-hydrogen shift through transition state **TS-8** (path II-2) or **TS-9** (path II-3), respectively. Vibrational frequency calculations show that **TS-7**, **TS-8**, and **TS-9** are real transition states, each with a single imaginary frequency on the singlet potential-energy surface. That is, the single imaginary frequency for each transition state (972*i* cm^{-1} for **TS-7**, 390*i* cm^{-1} for **TS-8**, and 1802*i* cm^{-1} for **TS-9**) provides a confirmation of an intramolecular isomerization process. The optimized transition-state structures (**TS-7**, **TS-8**, and **TS-9**) along with the calculated normal modes are shown in Figure 4. It is apparent that these transition states connect the singlet local minimum **Int-2** to the corresponding photoproducts **6** (1,3,6-heptatriene), **7** (norbornene), and **8** (4-methylenecyclohexene), respectively. These connections (between **Int-2** and corresponding photoproducts) have been verified by moving in both directions from transition states (**TS-7**, **TS-8**, and **TS-9**; Figure 1) along the intrinsic reaction coordinate.[13] Moreover, our computational findings suggest that these barrier heights decrease in the order **TS-8** (60 kcal/mol) > **TS-9** (18 kcal/mol) > **TS-7** (9.0 kcal/mol). In short, the path II mechanism of singlet photoisomerization of bicyclo[4,1,0]hept-2-ene **1** can be represented as follows:

$$1(S_0) + h\nu \rightarrow \text{FC-S} \rightarrow \text{CI-2} \rightarrow \text{Int-2} \rightarrow \text{TS-7} \rightarrow 6 \quad (5)$$

$$1(S_0) + h\nu \rightarrow \text{FC-S} \rightarrow \text{CI-2} \rightarrow \text{Int-2} \rightarrow \text{TS-8} \rightarrow 7 \quad (6)$$

$$1(S_0) + h\nu \rightarrow \text{FC-S} \rightarrow \text{CI-2} \rightarrow \text{Int-2} \rightarrow \text{TS-9} \rightarrow 8 \quad (7)$$

Furthermore, from the computational data discussed above, one can readily see that the barrier to path II-1 is the smallest (only 3.8 kcal/mol) among all of the reaction pathways. This finding suggests that path II-1 should be the most favorable from a kinetic viewpoint. On the basis of the present theoretical investigations as demonstrated in Figure 1, we thus predict that the photoproduct (1,3,6-heptatriene, **6**) produced by path II-1 should be in a larger quantum yield than the other photoproducts (**2**−**5**, **7**−**8**). This conclusion is in good agreement with the available experimental observations.[6]

2. Triplet Reaction Mechanisms of Bicyclo[4,1,0]hept-2-ene. Let us now turn to the triplet photoisomerization reactions of **1** (eq 2 in Scheme 1). Figure 5 displays the relative energies

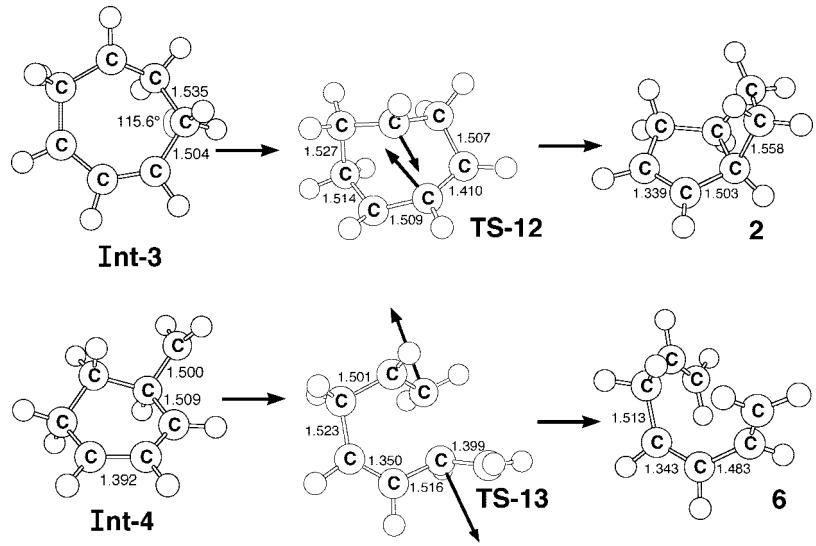

Figure 7. CAS(8,8)/6-311G(d) geometries (in angstroms and deg) for paths III and IV of bicyclo[4,1,0]hept-2-ene (**1**), intermediates (**Int-3** and **Int-4**), transition states (**TS-12** and **TS-13**) and isomer products (**2** and **6**, respectively). The heavy arrows indicate the main atomic motions in the transition state normal modes. For more information, see the Supporting Information.

on the triplet potential-energy surface along the assumed photoisomerization pathways from **1** to various photoproducts (**2** and **6**). Selected optimized geometrical parameters for the critical points of eq 2 and their energies on the ground- and lowest triplet-state surfaces can be taken from Figures 6 and 7, respectively. Cartesian coordinates calculated for the stationary and crossing points at the CASSCF/6-311G(d) level are available as Supporting Information.

Leigh and Srinivasan reported that the photochemistry of bicyclo[4,1,0]hept-2-ene **1** (2-norcarene) upon triplet-sensitized photolysis has been investigated.[6] They found that toluene-sensitized photolysis of **1** in deoxygenated pentane solution produced **2** and *cis*- and *trans*-**6** in yields that varied with the extent of photolysis. In the first step, the reactant (**1**) is excited to its lowest-lying triplet state (T_1) by a vertical excitation. After the vertical excitation process, the molecule is situated on the triplet surface but still possesses the ground-state (S_0) geometry. This point on the triplet surface is denoted as **FC-T** (T_1 (S_0 geometry)). The computed triplet vertical excitation energy of **1** is 95 kcal/mol ($S_0 \rightarrow T_1$ (S_0 geometry)). Comparison with the corresponding toluene sensitization experiments (3.605 eV $\approx$ 83 kcal/mol in energy)[6,12] indicates that the present calculations again provide a good estimate of the relative energies for the 2-norcarene system.

From the Franck−Condon point (**FC-T**), the molecule relaxes to a local minimum near to the S_0 geometry. This local minimum on the triplet surface is denoted **T_1-Rea-1** and is calculated to be about 61 kcal/mol above the ground-state minimum as demonstrated in Figure 5. The optimized geometrical parameters of **T_1-Rea-1** are given in Figure 6. Comparing the **T_1-Rea-1** geometry (Figure 6) with that of its corresponding ground-state minimum **1** (Figure 6), it is readily seen that the triplet state has significantly greater bond distances (i.e., C═C and C−C) than its closed-shell singlet state. The reason for this phenomenon can be understood simply by considering their respective electronic structures.[14]

From **T_1-Rea-1**, isomerization to the final photoproducts (**2** and **6**) involves two possible reaction pathways as demonstrated in Figure 5. Namely, on one hand, the system may undergo a cyclopropanic bond breaking between the C_1 and C_6 atoms via a transition state **TS-10** (path III). Alternatively, the reaction may proceed via cyclopropanic bond breaking between the C_1 and C_7 atoms, through a transition state **TS-11** (path IV). Vibrational frequency calculations show that both **TS-10** and **TS-11** are real transition states, each with a single imaginary frequency, on the triplet potential-energy surface. The optimized transition-state structures (**TS-10** and **TS-11**) along with the calculated normal modes are shown in Figure 6. It is apparent that these transition states connect the triplet local minimum **T_1-Rea-1** to the corresponding intersystem crossing points (**T_1/S_0-1** and **T_1/S_0-2**, respectively). The single imaginary frequency for each transition state (765*i* cm^{-1} for **TS-10** and 783*i* cm^{-1} for **TS-11**) provides a confirmation of a carbon−carbon bond breaking process. Again, the connections (between **T_1-Rea-1** and corresponding intersystem crossings) have been verified by moving in both directions from transition states (**TS-10** and **TS-11**; Figure 5) along the intrinsic reaction coordinate.[13]

Our MP2-CAS calculations suggest that formation of **T_1/S_0-1** from **T_1-Rea-1** proceeds via a transition state **TS-10** with a barrier of 16 kcal/mol, whereas **T_1/S_0-2** is formed through a transition state **TS-11** with a barrier of 12 kcal/mol. In consequence, from the reaction profiles shown in Figure 5, it is evident that this system has sufficient internal energy (34 kcal/mol) to overcome the energy barriers between the **T_1-Rea-1** minimum and the **T_1/S_0-1** (or **T_1/S_0-2**) intersection points after photoexcitation to the T_1 state (vide infra).

The optimized geometries and gradient difference vectors for **T_1/S_0-1** and **T_1/S_0-2** are illustrated in Figure 6. Basically, the structure of the **T_1/S_0-1** intersection point possesses a cycloheptene ring, with two unpaired electrons lying on the C_1 and C_6 atoms. On the other hand, the **T_1/S_0-2** intersection point has a methylcyclohexene structure, with two unpaired electrons located on the C_1 and C_7 atoms. It is obvious that these two unpaired electrons are far enough apart that their singlet and triplet states are degenerate. As a result, the T_1 and S_0 surfaces can intersect. Our theoretical investigations indicate that the **T_1/S_0-1** crossing point is located 36 kcal/mol below the **FC-T** point and 59 kcal/mol above the ground-state minimum, **1**. On the other hand, the **T_1/S_0-2** crossing point is located 28 kcal/mol below the **FC-T** point and 67 kcal/mol above the ground-state minimum, **1**. From these intersystem crossing points (**T_1/S_0-1** and **T_1/S_0-2**), the 2-norcarene (**1**) molecule may follow two kinds of reaction pathways (path III and path IV, respectively) as demonstrated in Figures 5 and 6. Accordingly, from an energetic

viewpoint, once reactant **1** has populated the T_1 state by photoexcitation, it would relax to the **T_1-Rea-1** minimum with sufficient internal energy to overcome barriers on the T_1 surface to reach one of the **T_1/S_0** intersection points. From here, ring closure and ring opening follow to yield the isomeric photoproducts (**2** and **6**). In short, the mechanisms of triplet photoisomerization of bicyclo[4,1,0]hept-2-ene **1** can be represented as follows:

$$1(S_0) + h\nu \rightarrow \text{FC-T} \rightarrow T_1\text{-Rea-1} \rightarrow \text{TS-10} \rightarrow T1/S_0\text{-1} \rightarrow \text{Int-3} \rightarrow \text{TS-12} \rightarrow 2 \quad (8)$$

$$1(S_0) + h\nu \rightarrow \text{FC-T} \rightarrow T_1\text{-Rea-1} \rightarrow \text{TS-11} \rightarrow T1/S_0\text{-2} \rightarrow \text{Int-4} \rightarrow \text{TS-13} \rightarrow 6 \quad (9)$$

As seen in Figure 5, the activation barrier of **TS-13** (via path IV) is apparently larger than that of **TS-12** (via path III). That is, the MP2-CAS calculations show that **TS-13** (20 kcal/mol) > **TS-12** (8.0 kcal/mol) with respect to the ground-state minimum **1**. Thus, our theoretical findings strongly suggest that path III is preferred over path IV. Accordingly, on the basis of the above computational results, one may then anticipate that, in the triplet photoisomerization of **1**, bicyclic **2** should be the predominant photoproduct. Our theoretical findings are in good accordance with the experimental observations as illustrated in Scheme 1.[6]

V. Conclusion

The photochemical reaction mechanisms of bicyclo[4,1,0]hept-2-ene **1** (2-norcarene) have been investigated in the present work. From this study, we can elaborate on the standard model of the photochemistry of **1**. In the singlet state, 2-norcarene is vertically excited to the S_1 state. Then, radiationless decay from S_1 to S_0 occurs via two conical intersections, which result in intramolecular photorearrangements. It should be mentioned that the variety of products formed has been grouped according to the 1,3-biradical intermediates (**Int-1** and **Int-2**) resulting from cleavage of the internal (C_1 and C_6) and external (C_1 and C_7) cyclopropane bonds. Starting from the conical intersection points, the products of the photoisomerizations can be reached on ground-state relaxation paths. These findings, based on the conical intersection viewpoint, have helped us to better understand the photochemical reactions and to support the experimental observations.[6] Also, we study the low-lying triplet photochemistry of **1** in this work. As one can see from the present study, the triplet mechanisms of **1** demonstrate similar reaction patterns as the corresponding singlet reactant. Moreover, our theoretical findings suggest that the computational results are in good agreement with the available experimental observations.[6]

Besides this, the present theoretical study demonstrates that substantial interaction occurs between nonconjugated olefin and cyclopropane moieties in the excited bicyclo[4,1,0]hept-2-ene (**1**) compound. That is, when this molecule absorbs light, it can produce an intramolecular electronic energy transfer from the double bond to the cyclopropane ring. The two chromophores are strongly coupled in the excited-state of **1**. Also, our theoretical findings indicate that, once bicyclo[4,1,0]hept-2-ene (**1**) absorbs light, it can undergo both cycloheptene ring expansion (path I or path III) and cyclohexene ring contraction (path II or path IV) mechanisms to obtain the various photoproducts. Both mechanisms involve an intramolecular electronic energy transfer from the double bond to the cyclopropane ring in the excited-state of **1**. That is, it was found that the double π bond absorbs the incident photon, whereas the reactions that are observed are mostly those of the cyclopropane ring.

It is hoped that the present work will stimulate further research into this subject.

Acknowledgment. The author is grateful to the National Center for High-Performance Computing of Taiwan for generous amounts of computing time, and the National Science Council of Taiwan for the financial support. The author also wishes to thank Professor Michael A. Robb, Dr. Michael J. Bearpark, (University of London, UK), and Professor Massimo Olivucci (Universita degli Sstudi di Siena, Italy) for their encouragement and support. Special thanks are also due to reviewer 1 and reviewer 2 for very helpful suggestions and comments.

Supporting Information Available: Geometries calculated with the CASSCF(8,8)/6-311G* basis set. This material is available free of charge via the Internet at http://pubs.acs.org.

References and Notes

(1) For reviews, see. (a) Leigh, W. J.; Srinivasan, R. *Acc. Chem. Res.* **1987**, *20*, 107. (b) Hixson, S. S. *Organic Photochemistry*; Padwa, A., Ed.; Marcel Dekker: New York, 1979; Vol. 4, pp 218−260.

(2) Srinivasan, R.; Ors, J. A. *J. Org. Chem.* **1979**, *44*, 3426.

(3) (a) Srinivasan, R.; Ors, J. A. *J. Am. Chem. Soc.* **1978**, *100*, 7089. (b) Srinivasan, R.; Ors, J. A.; Baum, T. *J. Org. Chem.* **1981**, *46*, 1950. (c) Srinivasan, R.; Baum, T.; Ors, J. A. *Tetrahedron Lett.* **1981**, *22*, 4795.

(4) (a) Srinivasan, R.; Ors, J. A.; Brown, K. H.; Baum, T.; White, L. S.; Rossi, A. R. *J. Am. Chem. Soc.* **1980**, *102*, 5297. (b) Leigh, W. J.; Srinivasan, R. *J. Org. Chem.* **1983**, *48*, 3970.

(5) (a) Srinivasan, R.; Ors, J. A. *J. Am. Chem. Soc.* **1979**, *101*, 3411. (b) Srinivasan, R.; Baum, T.; Brown, K. H.; Ors, J. A.; White, L. S.; Rossi, A. R.; Epling, G. A. *J. Chem. Soc., Chem. Commun.* **1981**, 973.

(6) Srinivasan, R.; Leigh, W. J. *J. Am. Chem. Soc.* **1983**, *105*, 514.

(7) For instance, as pointed out by the same authors, according to deuterium-labeling studies, the dominant photoproduct, *cis*-1,3,6-heptatriene, is formed via formal electrocyclic [$2\pi + 2\omega + 2\sigma$] ring opening of the bicyclo[4,1,0]hept-2-ene ring system in a manner analogous to the 1,3-cyclohexadiene/1,3,5-hexatriene interconversion; see ref 6.

(8) (a) Bernardi, F.; Olivucci, M.; Robb, M. A. *Isr. J. Chem.* **1993**, 265. (b) Klessinger, M. *Angew. Chem., Int. Ed. Engl.* **1995**, *34*, 549. (c) Bernardi, F.; Olivucci, M.; Robb, M. A. *Chem. Soc. Rev.* **1996**, 321. (d) Bernardi, F.; Olivucci, M.; Robb, M. A. *J. Photochem. Photobiol., A* **1997**, *105*, 365. (e) Klessinger, M. *Pure Appl. Chem.* **1997**, *69*, 773. (f) Klessinger, M.; Michl, J. In *Excited States and Photochemistry of Organic Molecules*; VCH Publishers: New York, 1995.

(9) Frisch, M. J.; Trucks, G. W.; Schlegel, H. B.; Scuseria, G. E.; Robb, M. A.; Cheeseman, J. R. ; Montgomery J. A., Jr.; Vreven, T.; Kudin, K. N.; Burant, J. C.; Millam, J. M.; Iyengar, S. S.; Tomasi, J.; Barone, V.; Mennucci, B.; Cossi, M.; Scalmani, G.; Rega, N.; Petersson, G. A.; Nakatsuji, H.; Hada, M.; Ehara, M.; Toyota, K.; Fukuda, R.; Hasegawa, J.; Ishida, M.; Nakajima, T.; Honda, Y.; Kitao, O.; Nakai, H.; Klene, M.; Li, X.; Knox, J. E.; Hratchian, H. P.; Cross, J. B.; Bakken, V.; Adamo, C.; Jaramillo, J.; Gomperts, R.; Stratmann, R. E.; Yazyev, O.; Austin, A. J.; Cammi, R.; Pomelli, C.; Ochterski, J. W.; Ayala, P. Y.; Morokuma, K.; Voth, G. A.; Salvador, P.; Dannenberg, J. J.; Zakrzewski, V. G.; Dapprich, S.; Daniels, A. D.; Strain, M. C.; Farkas, O.; Malick, D. K.; Rabuck, A. D.; Raghavachari, K.; Foresman, J. B.; Ortiz, J. V.; Cui, Q.; Baboul, A. G.; Clifford, S.; Cioslowski, J.; Stefanov, B. B.; Liu, G.; Liashenko, A.; Piskorz, P.; Komaromi, I.; Martin, R. L.; Fox, D. J.; Keith, T.; Al-Laham, M. A.; Peng, C. Y.; Nanayakkara, A.; Challacombe, M.; Gill, P. M. W.; Johnson, B.; Chen, W.; Wong, M. W.; Gonzalez, C.; Pople, J. A. *Gaussian 03*; Gaussian, Inc.: Wallingford, CT, 2004.

(10) Dunning, T. H., Jr.; Hay, P. J. In *Modern Theoretical Chemistry*; Schaefer, H. F., III, Ed.; Plenum: New York, 1976; pp 1−28.

(11) Bearpark, M. J.; Robb, M. A.; Schlegel, H. B. *Chem. Phys. Lett.* **1994**, *223*, 269.

(12) Swiderek, P.; Michaud, M.; Sanche, L. *J. Chem. Phys.* **1996**, *105*, 6724.

(13) Jensen, F. In *Introduction to Computational Chemistry*, 2nd ed.; Wiley: Chichester, U.K., 2007.

(14) Because the excited electron occupies the antibonding orbital, this can make a longer bond distance. Also see: Jorgensen, W. L.; Salem, L. *The Organic Chemist's Book of Orbitals*; Academic Press: New York, 1973.

JP803365U